Theoret. Chim. Acta (Berl.) 41, 223-232 (1976)

Electronic and Magnetic Structure of the Polymeric System Di-Imidazolato Iron(II)*

I. Mössbauer Spectroscopy and Thermogravimetry

Hans-E. Marcolin, Alfred Trautwein, Yutaka Maeda**

Fachbereich für Angewandte Physik, Universität des Saarlandes, Saarbrücken

Fritz Seel, Peter Wende

Fachbereich für Anorganische und Physikalische Chemie, Universität des Saarlandes, Saarbrücken

Received September 25, 1975/December 24, 1975

The polymeric system di-imidazolato iron(II) is synthesized from the reaction of either ferrocene or cyclopentadienyl-irondicarbonyl with imidazole. From Mössbauer measurements in the temperature range 4.2 K $\leqslant T \leqslant$ 448 K we find two different iron sites in the compound, denoted by A and B, respectively with ratio $[A]/[B] = 1.79 \pm 0.03$. From the isomer shift values we conclude that both Fe^A and Fe^B are in the ferrous high-spin state. Below 13.95 ± 0.10 K both subspectra are considerably broadened due to magnetic ordering. From the analysis of the magnetic spectra we derive for the main component V_{zz} of the electric field gradient tensor $V_{zz}^A > 0$ and $V_{zz}^B < 0$. Additionally, we investigate the thermal decomposition of the compound by thermogravimetry in the temperature range 20 °C $\leqslant T \leqslant$ 750 °C and by Mössbauer spectroscopy in the temperature range 20 °C $\leqslant T \leqslant$ 505 °C. The decomposition takes place in four steps. The first step between 20 °C and 190 °C is due to the loss of imidazole non-bonded to iron(II). Comparing the amount of iron with that of pure imidazolato iron(II) we find the formula $FeIz_2 + 0.70\ (\pm 0.02)$ IzH, with Iz standing for doubly deprotonated and IzH for deprotonated imidazole. Step 2 (193 °C $< T <$ 235 °C) and step 3 (400 °C $< T <$ 500 °C) are found from both methods. Step 4 is above 500 °C. Heat treatment and vacuum conditions affect the thermal decomposition products.

Isomer shifts δ^A and δ^B, and temperature dependent quadrupole splittings ΔE_Q^A and ΔE_Q^B are explained using a simple ligand field picture for orbital splittings and occupancies of quasi-tetrahedrally (A) and quasi-octahedrally (B) coordinated ferrous high-spin compounds. Using finally the experimental ratio $[A]/[B] = 1.79$ we derive for the over-all chemical formula

$$(1.79\ Fe^A Iz_{4/2} + Fe^B Iz_{4/2} + 2\ IzH)_n = (FeIz_2 + 0.71\ Iz)_n$$

in agreement with the result which we derived from investigating the thermal decomposition of our compound.

Key words: Mössbauer spectroscopy – Thermogravimetry – Di-imidazolato iron(II)

1. Introduction

So far only a few aza-homologues of the various metal complexes of cyclic polymethines are known [1]. Seel *et al.* [2] recently succeeded to derive imidazolato iron(II) with excess imidazole, $FeIz_2 \cdot x$ IzH ($x = 0.5$), from a reaction of

* Supported by Deutsche Forschungsgemeinschaft

** Present address: Research Reactor Institute, Kyoto University, Japan

either ferrocene or cyclopentadienylirondicarbonyl with imidazole. Applying an analogous procedure it was possible to get Fe-compounds with doubly deprotonated imidazole groups as ligands [3]. In the following we study the influence of the 2-position of the heterocyclic ring upon stoichiometry and structure of the new compound. As a first step in the present communication we investigate $FeIz_2 \cdot x$ IzH by thermogravimetric and Mössbauerspectroscopic methods. Then we continue to discuss in a succeeding paper [4] the systems FeL_2 – with L standing for 2-methyl-, 2-ethyl-, and 2-phenyl-imidazole, respectively.

2. Materials

For the preparation of $FeIz_2 \cdot x$ IzH the reaction of either ferrocene or cyclopentadienylirondicarbonyl in the melt of the heterocyclic system seems most favourable. The reaction products are quite sensitive to the influence of atmosphere and moisture and therefore have to be handled in vacuum, dry inert gas, or N_2 atmosphere.

The reaction of ferrocene with imidazole is necessarily carried out in a sealed glass tube, since sublimation of $Fe(C_5H_5)_2$ is faster than the desired reaction itself. After the heterocyclic system is melted we first get a red solution of ferrocene which then becomes transparent with simultaneous precipitation of brown crystals of $FeIz \cdot x$ IzH. The whole reaction is of practical use only above 180 °C, probably due to the high stability of ferrocene.

The decomposition of cyclopentadienylironcarbonyl and subsequent reaction with imidazole starts already at lower temperatures (compared with 180 °C), because the carbonyl complex is less stable than ferrocene. After melting of the heterocyclic system we first get a red solution of $[C_5H_5Fe(CO)_2]_2$ in imidazole which then on increasing the temperature becomes transparent with simultaneous precipitation of brown crystals of Fe(II) imidazolyl and formation of carbonmonoxide.

For both types of reaction we used an excess amount of imidazole. Thus each final probe contained excess imidazole to varying degrees, which can be removed by sublimation.

A more detailed description of the preparation of imidazolato iron(II) complexes and analytical data is given elsewhere [5].

3. Mössbauer Results in the Temperature Range 4.2 K $\leqslant$ T $\leqslant$ 448 K

For low-temperature measurements $FeIz_2 \cdot x$ IzH polycrystalline powder was filled under N_2-atmosphere into an absorber holder (Cu) yielding a sample with an approximate thickness of 0.5 mm and a diameter of 10 mm. The sample was shielded from atmosphere or exchange gas in the cryostat by indium-sealed mylar windows. For high-temperature measurements (>300 K) new sample material was filled under N_2-atmosphere into an absorber holder (Cu) which was open on one side and closed on the other by an Al window, thus exposing the probe to vacuum in the furnace (Elscint, type RICOR). The effective sample area was only 12.56 mm^2 in this case. With this geometry we were able to keep the temperature

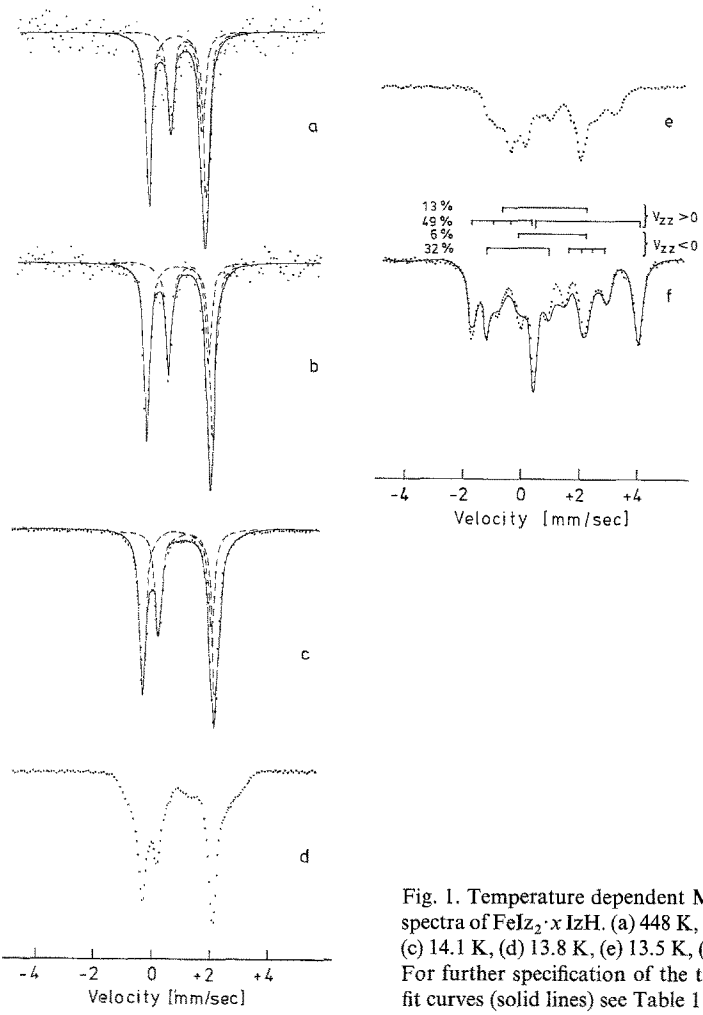

Fig. 1. Temperature dependent Mössbauer spectra of $FeIz_2 \cdot x$ IzH. (a) 448 K, (b) 300 K, (c) 14.1 K, (d) 13.8 K, (e) 13.5 K, (f) 11.5 K. For further specification of the theoretical fit curves (solid lines) see Table 1

gradient smaller than 1 °C mm^{-1} even at 500 °C. The 300 K measurement of the material exposed to vacuum (10^{-4} Torr) in the furnace yielded the same spectrum as that obtained from a 300 K measurement of another sample which was built into the cryostat for low-temperature studies.

In Fig. 1 we show some of the spectra obtained in the temperature range $11.5\ K \leqslant T \leqslant 448\ K$, and we find from spectrum a that we are concerned with two different iron sites, denoted by A and B, respectively. This finding was checked by investigation of four samples, each derived from different preparations and all four yielding identical Mössbauer spectra. Table 1 contains isomer shifts δ, quadrupole splittings ΔE_Q and area ratios $[A]/[B]$ which we derive from least square computer fits of the experimental data. Below $T = 13.95 \pm 0.10$ K magnetic ordering within the sample broadens the absorption lines (Fig. 1 d, e) leading to a well-resolved magnetic hyperfine pattern at 11.5 K (Fig. 1 f). For this temperature

Table 1. Isomershifts δ, quadrupole splittings ΔE_Q, area ratios $[A]/[B]$, internal magnetic fields H^{int} of the two sites A and B in $FeIz_2 \cdot x$ IzH at various temperatures T

T(K)	Site	δ(mm sec^{-1})[a]	ΔE_Q(mm sec^{-1})	$[A]/[B]$	H^{int}(kG)	Time of measurement	Fig.
448	*A*	0.663±0.007	1.870±0.005	1.77	paramag.	2 h	1a
	B	0.956±0.009	0.999±0.008	±0.03			
423	*A*	0.703±0.007	1.935±0.005	1.76	paramag.	1 h	
	B	0.978±0.009	1.065±0.008	±0.03			
373	*A*	0.703±0.007	2.109±0.005	1.78	paramag.	20 min	
	B	0.999±0.009	1.152±0.008	±0.03			
300	*A*	0.746±0.005	2.289±0.003	1.792	paramag.	2 h	1b
	B	1.046±0.008	1.421±0.005	±0.015			
77	*A*	0.882±0.004	2.416±0.003	1.778	paramag.	5 h	
	B	1.203±0.007	1.973±0.004	±0.015			
14.1	*A*	0.909±0.005	2.459±0.003	1.779	paramag.	5 h	1c
	B	1.159±0.008	1.863±0.005	±0.015			
13.8	transition state					5 h	1d
13.5	transition state					15 h	1e
11.5[b]	*A*	0.909	2.459	13%	paramag.	15 h	1f
		0.84	2.91	51%	112.6		
	B	1.159	1.863	6% 1.78	paramag.		
		1.09	2.36	30%	66.1		

[a] Isomer shifts are given relatively to metallic iron at room temperature.

[b] The theoretical spectrum (solid line in Fig. 1d) contains the assumption:
(1) the values for the paramagnetic subspectra are taken from the 14.1 K-spectrum;
(2) the asymmetry parameter η is zero;
(3) the main component of the electric field gradient tensor (V_{zz}) is parallel to H^{int}
(4) $V_{zz}^A > 0$, and $V_{zz}^B < 0$.

we calculate an overall spectrum (solid line in Fig. 1 f) consisting of four subspectra as indicated by the stick spectra in Fig. 1 f and as specified in Table 1. It turns out that a reasonable fit of the experimental data at 11.5 K is only possible assuming some remaining paramagnetic contribution, i.e. ca. 15% for the *A*-site and ca. 5% for the *B*-site. This result seems plausible under the aspect that the compound undergoes a crystallographic change below $T = 13.95$ K. The sudden increase of ΔE_Q^A and ΔE_Q^B in the magnetic region with respect to the quadrupole splittings in the paramagnetic region seems to support this assumption. Similar broad magnetic-paramagnetic transition accompanied by a crystallographic distortion was reported previously for Rb_2FeF_4 [6]. An alternative explanation for the fact that ΔE_Q^A and ΔE_Q^B abruptly are increased in the magnetic phase, however, might be given under the aspect of a magnetically induced quadrupole splitting [7]. The type of magnetic ordering will be discussed in the succeeding paper [4].

Fig. 2 shows the effect of applying an external magnetic field, H^{ext}, perpendicular to the γ-beam at 77 K (a: $H^{ext} = 0$; B: $H^{ext} = 47.3$ kG). The solid curve in Fig. 2b results from computer analysis, described in detail by Gabriel *et al.* [8], using the δ- and ΔE_Q-values from Table 1 for 77 K, and additionally $H^{int} = -15$ kG, $H^{ext} = 47.3$ kG, $H^{ext} \perp \gamma$, $V_{zz}^A > 0$, and $V_{zz}^B < 0$. The assumption that the internal field is *nearly* zero at 77 K under the application of an external magnetic field is reasonable even for ferrous high-spin compounds, since the thermal average of the electronic

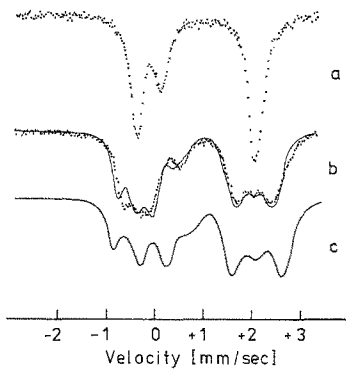

Fig. 2. Mössbauer spectra of $FeIz_2 \cdot x$ IzH at 77 K. (a) $H^{ext}=0$, (b) $H^{ext}=47.3$ kG perpendicular to γ-beam; theoretical spectrum (solid line) was calculated with the $\delta^{A,B}$ and $\Delta E_Q^{A,B}$ values of Table 1, with $H^{int}=-15$ kG, $H^{ext}=47.3$ kG, $H^{ext}\perp\gamma$, $V_{zz}^{A}>0$, $V_{zz}^{B}<0$, and $[A]/[B]=1.78$, (c) Theoretical spectrum with the same values as in (b) but $H^{int}=0$

spin, $\langle S\rangle_T$, becomes zero at elevated temperatures [9]. For comparison we give in Fig. 2c the theoretical spectrum for $H^{int}=0$ ($\langle S\rangle_T=0$). From the magnetic spectra at 77 K we find for the sign of $V_{zz}^{A,B}$ the same result as from the spectrum at 11.5 K (Table 1).

4. Thermal Decomposition

The thermal decomposition of $FeIz_2 \cdot x$ IzH we investigated by means of thermogravimetry and Mössbauer spectroscopy. Fig. 3 shows the loss of mass depending on the heat treatment under vacuum (<0.1 Torr); the temperature was increased by 0.5 degrees per minute during the thermogravimetry measurement.

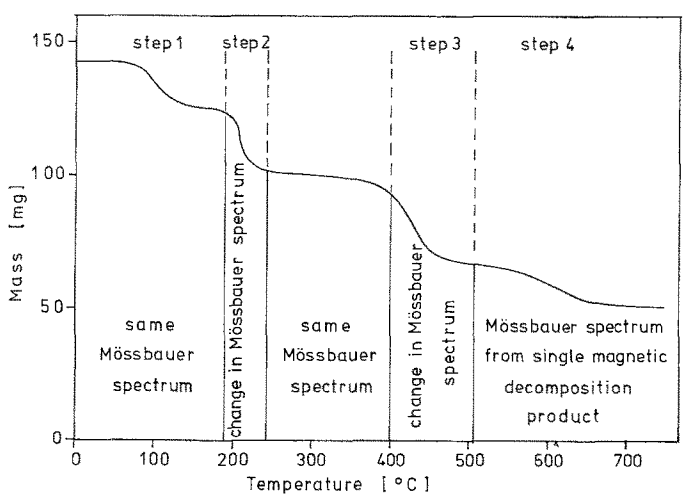

Fig. 3. Thermal decomposition of $FeIz \cdot x$ IzH

This procedure was carried out twice with different samples leading to the same result. From Fig. 3 it follows that the complex is decomposed in mainly four steps with constant mass above 700 °C. From the chemical analysis of the remaining material above 700 °C we find that it consists partly of metallic iron and partly of decomposition products which we were not able to identify.

For comparison we measured a series of about 60 Mössbauer spectra from two samples which were exposed to vacuum in an Elscint-furnace as described in section 3.

As a first step we collected data at room temperature, 100 °C, 150 °C, and 175 °C leading to the results which we already specified in Fig. 1a and Table 1. Since the area ratio $[A]/[B]$ does not change within the error range by heating the sample from room temperature to 175 °C, we conclude that step 1 in the thermal decomposition curve of Fig. 3, obtained by thermogravimetry, is due to the loss of imidazole non-bonded to iron(II) in the compound (note that the material was synthesized using an excess amount of imidazole; section 2). At 200 °C we measured for two hours without getting any spectrum, whereas measuring at 175 °C for two hours yielded a useful spectrum, (Fig. 1a); this indicates that the material starts to decompose at around 200 °C, in agreement with step 2 of Fig. 3. The spectrum of the decomposition product, which resulted from the heat treatment at 200 °C for two hours, was then measured after the sample had been cooled down to room-temperature but kept under vacuum in the furnace (Fig. 4). The fit of this spectrum with four quadrupole patterns is arbitrary, however; it indicates that we are still concerned with relatively high isomer shift values of about 0.75 mm/sec with respect to metallic iron. This spectrum did not change after keeping the sample for 20 minutes at temperatures of 225 °C, 250 °C, 275 °C, and 300 °C, respectively, and measuring at the end of each heat treatment at room-temperature. This result is in agreement with the horizontal part of the thermal decomposition curve of Fig. 3 between 200 °C and 300 °C.

In order to simulate the conditions of the thermogravimetry experiment more closely, we used an additional sample and investigated its thermal decomposition in 29 steps within the temperature range $20\ °C \leqslant T' \leqslant 505\ °C$. At each specific temperature T' we kept the sample for 30 minutes and then cooled it back to room temperature, i.e. all spectra were taken at room temperature. Fig. 5 shows some

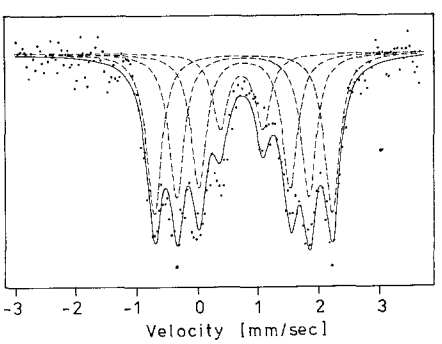

Fig. 4. Mössbauer spectrum of FeIz·x IzH at room temperature after keeping the sample for two hours in vacuum (10^{-4} Torr) at 200 °C

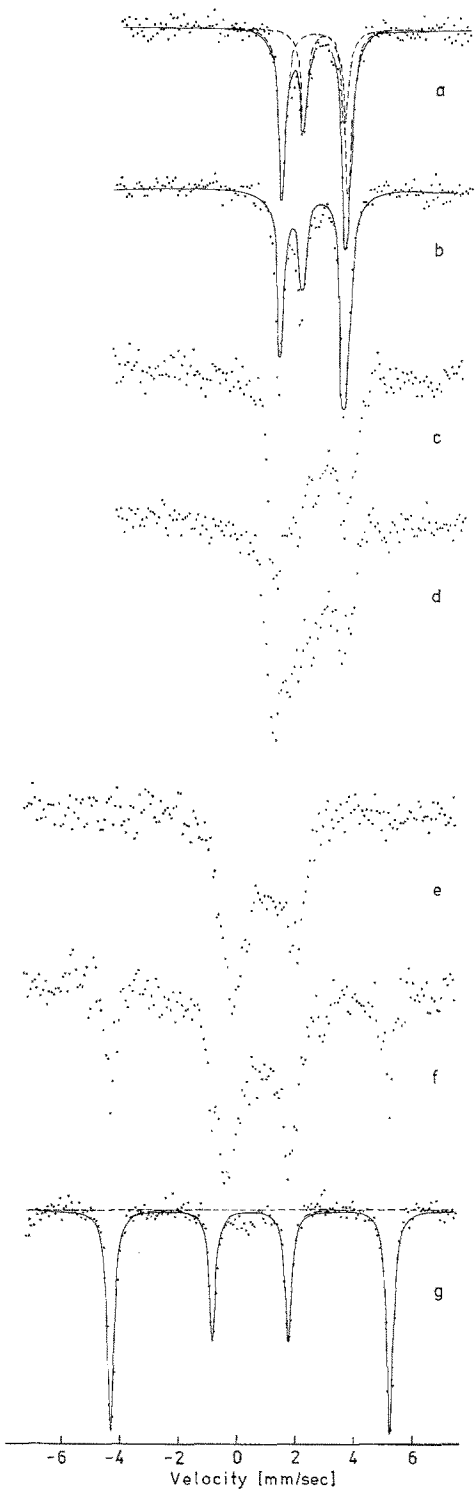

Fig. 5. Mössbauer spectra of $FeIz_2 \cdot x$ IzH at room temperature after keeping the sample for 30 minutes in vacuum (10^{-4} Torr) at temperatures (a) 193 °C, (b) 201 °C, (c) 235 °C, (d) 242 °C, (e) 400 °C, (f) 461 °C, and (g) 505 °C. The solid curves in (a) and (b) correspond to $\delta^{A,B}$- and $\Delta E_Q^{A,B}$-values specified in Table 1 for the 300 K measurement. The solid line in (g) represents the γ-Fe_2O_3 spectrum with $\delta = 0.453 \pm 0.008$ mm sec^{-1}, $\Delta E_Q = 0.50 \pm 0.03$ mm sec^{-1}, and $H^{int} = 508 \pm 2$ kG. The outermost resonance lines in this magnetic spectrum are missing due to the relatively small velocity used in this series of measurement

spectra out of this cycle. The $T' = 193$ °C spectrum (Fig. 5a) is found to be identical with the room temperature spectrum. At $T' = 201$ °C (Fig. 5b) we already see some deviation from the $T' = 193$ °C spectrum, which for comparison is given as the solid curve in Fig. 5b. The increase of T' to 235 °C (Fig. 5c) further decomposes the sample, leading to a spectrum at $T' = 242$ °C (Fig. 5d) which remains nearly constant up to $T' = 400$ °C (Fig. 5e). Above $T' = 400$ °C the next step in thermal decomposition starts, with already a remarkable amount of magnetic material at $T' = 461$ °C (outer line in Fig. 5f). At $T' = 505$ °C (Fig. 5g) all of the original sample is converted into a magnetic compound, which we analyzed from our computer fit (solid curve in Fig. 5g) as γ-Fe_2O_3, with the characteristic parameters of $\delta = 0.452 \pm 0.008$ mm sec^{-1}, $\Delta E_Q = 0.5 \pm 0.03$ mm sec^{-1}, and $H^{\text{int}} = 508 \pm 2$ kG. It is not surprising that our final decomposition product is an iron oxide, since the relatively weak vacuum of 10^{-4} Torr in our furnace and the smooth thermal decomposition during an overall time-period of three weeks reveals enough oxygen for a reaction with iron.

Comparing thermogravimetric results and Mössbauer results obtained from the thermal decomposition study of $FeIz_2 \cdot x$ IzH we draw the following conclusions:

(1) Step 1 of Fig. 3 is due to the loss of imidazole non-bonded to iron(II).

(2) Comparing the amount of iron with that of di-imidazolato iron(II) at $T' =$ 193 °C we find from two different series of thermal decomposition the formula $FeIz_2 \cdot 0.70$ IzH, with an uncertainty in the factor 0.70 of ± 0.02.

(3) Steps 2 and 3 of Fig. 3 are reproduced by a series of Mössbauer spectra in the temperature range 200 °C $< T <$ 505 °C.

(4) Heat treatment (time and temperature) and vacuum conditions affect the thermal decomposition products.

5. Discussion

For the further discussion of the chemical structure of $FeIz_2 \cdot 0.70$ IzH we use the isomer shift values, quadrupole splittings, and area ratio $[A]/[B]$ in Table 1 for the temperature range 14.1 K $\leqslant T \leqslant$ 448 K.

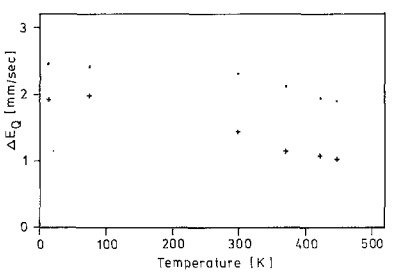

Fig. 6. Temperature dependence of quadrupole splittings in $FeIz_2 \cdot x$ IzH. $(\cdot)\Delta E_Q^A(T)$, $(+)\Delta E_Q^B(T)$. Note that the error limits of the experimental prints are much smaller than the symbols $(\cdot)$ and $(+)$

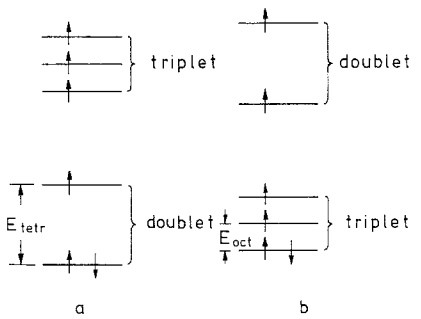

Fig. 7. One-electron orbital splittings and occupancies for Fe 3*d* electrons in (a) quasi-tetrahedrally and (b) quasi-octahedrally coordinated ferrous high-spin compounds

From the relatively large isomer shifts and quadrupole splittings which we find for both the *A*- and *B*-subspectra it is obvious [10] that we are concerned with ferrous high-spin iron in both cases. For the interpretation of the temperature dependence of ΔE_Q^A and ΔE_Q^B (Fig. 6) we use the rough ligand field picture that quasi-tetrahedral and quasi-octahedral ferrous high-spin compounds are characterized by Fe 3*d* orbital splittings and occupancies as shown in Fig. 7a and 7b, respectively. With typical energy separations $E_{oct} < E_{tetr}$ [11] we are concerned with a pronounced temperature dependence of ΔE_Q^B between transition temperature (13.95 ± 0.10 K) and room temperature, while ΔE_Q^A is less affected by temperature within this range (above 300 K, when kT comes closer to E_{tetr}, it is obvious that ΔE_Q^A will be affected stronger by increasing temperature than in the limit $kT \ll E_{tetr}$). The specific behavior of the *B*-site with an increase and subsequent decrease of ΔE_Q^B with increasing temperature was also found in another quasi-octahedrally coordinated ferrous high-spin compound [7] (α-$FeSO_4$). Additionally the δ values also reflect the situation for the *A*- and *B*-sites; ferrous high-spin halides, for example, show significantly smaller isomer shifts in tetrahedrally coordinated compounds compared with octahedrally coordinated compounds [10]. Thus we derive that (1) Fe^A is related to iron in a distorted tetrahedron of four neighboring imidazole groups, and (2) Fe^B is related to iron in a distorted octahedron of six neighboring imidazole groups.

This conclusion is further supported by considering the over-all chemical formula of the polymer: (1) The tetrahedrally coordinated iron is characterized by $(Fe^A Iz_{4/2})_n$; each imidazole is shared by two irons. (2) The octahedrally coordinated iron is bound to four imidazole groups with each shared by two irons, and the remaining two coordinations are occupied by two imidazole groups which belong only to the *B*-type iron. In this case the second imidazole-nitrogen is coupled with a proton, denoted by IzH. For the *B*-type iron then we are concerned with $(Fe^B Iz_{4/2} + 2\ IzH)_n$. Taking finally account of the experimental ratio $[A]/[B] = 1.79$ from Table 1, we find the over-all chemical formula

$$(1.79\ Fe^A Iz_{4/2} + Fe^B Iz_{4/2} + 2\ IzH)_n = (FeIz_2 + 0.71\ IzH)_{\bar{n}}$$

in agreement with the result we derived from our thermal decomposition study.

The uncertainty in the ratio $[A]/[B]$ from Table 1 is comparable with the error in the formula $FeIz_2 + 0.70\ (\pm 0.02)\ IzH$.

Our present structure result for di-imidazolato iron(II) with excess imidazole is especially interesting with respect to the structure of the Co-imidazole adduct, which was found from X-ray analysis [12] to consist only of tetrahedrally coordinated Co.

References

1. Pauson,P.L., Joshi,K.K., Qazi,A.R., Stubbs,W.H.: J. Organomet. Chem. **1**, 471 (1964)
2. Seel,F., Sperber,V.: Angew. Chem. **80**, 38 (1968)
3. Wende,P.: Diplomarbeit, Fachbereich 13.1, Universität des Saarlandes (1974)
4. Trautwein,A., Maeda,Y., Seel,F., Wende,P.: this volume.
5. Seel,F., Wende,P., Trautwein,A., Marcolin,H.E., Maeda,Y.: Z. Anorg. Chem., in press
6. Wertheim,G., Guggenheim,H.J., Levinstein,H.J., Buchanan,O.N.E., Sherwood,C.R.: Phys. Rev. **173**, 614 (1968)
7. Zimmermann,R., Trautwein,A.: Phys. Rev. **B12**, 3902 (1975)
8. Gabriel,J.R., Olsen,D.: Nucl. Instr. Meth. **70**, 209 (1969); Gabriel,J.R., Ruby,S.L.: Nucl. Instr. Meth. **36**, 23 (1965)
9. Trautwein,A.: Structure and Bonding **20**, 101 (1974)
10. Greenwood,N.N., Gibb,T.C.: Mössbauer spectroscopy. London: Chapman and Hall 1971
11. Orgel,L.E.: An introduction to transition-metal chemistry. New York: Wiley 1967
12. Seel,F., Hoppe,W.: unpublished results

Prof. Dr. A. Trautwein
Universität des Saarlandes
Fachbereich 12.1
Werkstoffphysik und Werkstofftechnologie
D-6600 Saarbrücken
Federal Republic of Germany